

1 SEARCH FOR PRODUCTION OF A HIGGS BOSON AND A SINGLE TOP  
2 QUARK IN MULTILEPTON FINAL STATES IN  $pp$  COLLISIONS AT  $\sqrt{s} = 13$   
3 TeV.

4 by

5 Jose Andres Monroy Montañez

6 A DISSERTATION

7 Presented to the Faculty of

8 The Graduate College at the University of Nebraska

9 In Partial Fulfilment of Requirements

10 For the Degree of Doctor of Philosophy

11 Major: Physics and Astronomy

12 Under the Supervision of Kenneth Bloom and Aaron Dominguez

13 Lincoln, Nebraska

14 July, 2018

15 SEARCH FOR PRODUCTION OF A HIGGS BOSON AND A SINGLE TOP  
16 QUARK IN MULTILEPTON FINAL STATES IN pp COLLISIONS AT  $\sqrt{s} = 13$   
17 TeV.

18 Jose Andres Monroy Montañez, Ph.D.

19 University of Nebraska, 2018

20 Adviser: Kenneth Bloom and Aaron Dominguez

# Table of Contents

22	<b>Table of Contents</b>	<b>iii</b>
23	<b>List of Figures</b>	<b>iv</b>
24	<b>List of Tables</b>	<b>v</b>
25	<b>5 Statistical methods</b>	<b>1</b>
26	5.1 Multivariate analysis . . . . .	1
27	5.1.1 Decision trees . . . . .	5
28	5.1.2 Boosted decision trees (BDT). . . . .	7
29	5.1.3 Overtraining . . . . .	10
30	5.1.4 Variable ranking . . . . .	10
31	5.1.5 BDT output example. . . . .	11
32	5.2 Statistical inference. . . . .	12
33	5.2.1 Nuisance parameters. . . . .	12
34	5.2.2 Maximum likelihood estimation method . . . . .	13
35	5.3 Upper limits . . . . .	15
36	<b>Bibliography</b>	<b>18</b>
37	<b>References</b>	<b>20</b>

## 38 List of Figures

39	5.1	Scatter plots-MVA event classification. . . . .	3
40	5.2	Scalar test statistical. . . . .	4
41	5.3	Decision tree. . . . .	5
42	5.4	Decision tree output example. . . . .	8
43	5.5	BDT output example. . . . .	11
44	5.6	$t_r$ p.d.f. assuming each $H_0$ and $H_1$ . . . . .	16
45	5.7	Illustration of the $CL_s$ limit. . . . .	17
46	5.8	Example of Brazilian flag plot . . . . .	19

## <sup>47</sup> List of Tables

## 48 Chapter 5

### 49 Statistical methods

50 In the course of analyzing the data sets provided by the CMS experiment and used in  
51 this thesis, several statistical tools have been employed; in this chapter, a description  
52 of these tools will be presented, starting with the general statement of the multivariate  
53 analysis methods, followed by the particularities of the Boosted Decision Trees (BDT)  
54 method and its application to the classification problem. Statistical inference methods  
55 used will also be presented. This chapter is based mainly on References [126–128].

#### 56 5.1 Multivariate analysis

57 Multivariate data analysis (MVA) makes use of the statistical techniques developed  
58 to analyze more than one variable at once, taking into account all the correlations  
59 among variables. MVA is employed in a variety of fields like consumer and market  
60 researches, quality control and process optimization. Using MVA it is possible to  
61 identify the dominant patterns in a data sample, like groups, outliers and trends, and  
62 determine to which group a set of values belong; in the particle physics context, MVA  
63 methods are used to perform the selection of certain type of events from a large data

64 set, e.g., a raw data input.

65 Processes with small cross section, such as the  $tHq$  process, are hard to detect  
 66 in the presence of the processes with larger cross sections; therefore, only a small  
 67 fraction of the data contains events of interest (signal), the major part is signal-like  
 68 events, which mimic signal characteristics but belong to different process, so they are  
 69 a background to the process of interest. This implies that it is not possible to say  
 70 with certainty that a given event is a signal or a background and statistical methods  
 71 should be involved. In that sense, the challenge can be formulated as one where a  
 72 set of events have to be classified according to certain special features; these features  
 73 correspond to the measurements of several parameters like energy or momentum,  
 74 organized in a set of *input variables*. The measurements for each event can be written  
 75 in a vector  $\mathbf{x} = (x_1, \dots, x_n)$  for which

- 76 •  $f(\mathbf{x}|s)$  is the probability density (*likelihood function*) that  $\mathbf{x}$  is the set of mea-  
 77 sured values given that the event is a signal event (signal hypothesis).
- 78 •  $f(\mathbf{x}|b)$  is the probability density (*likelihood function*) that  $\mathbf{x}$  is the set of mea-  
 79 sured values given that the event is a background event (background hypothe-  
 80 sis).

81 Figure 5.1 shows three ways to perform a classification of events for which mea-  
 82 surements of two properties, i.e., two input variables  $x_1$  and  $x_2$ , have been performed;  
 83 blue circles represent signal events while red triangles represent background events.  
 84 The classification on the left is *cut-based* requiring  $x_1 < c_1$  and  $x_2 < c_2$ ; usually the cut  
 85 values ( $c_1$  and  $c_2$ ) are chosen according to some knowledge about the event process.  
 86 In the middle plot, the classification is performed using a linear function of the input  
 87 variables, hence the boundary is a line, while in the right plot the the relationship  
 88 between input variables is not linear thus the boundary is not linear either.

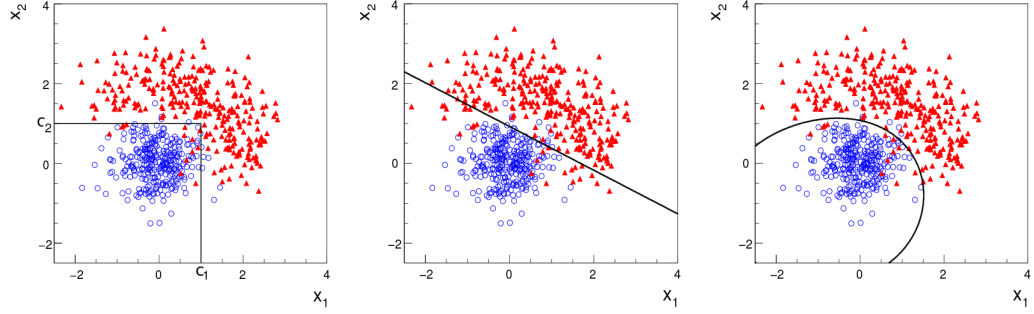


**Figure 5.1:** Scatter plots-MVA event classification. Distribution of two input variables  $x_1$  and  $x_2$  measured for a set of events; blue circles represent signal events and red triangles represent background events. The classification is based on cuts (left), linear boundary (center), and nonlinear boundary (right) [126]

89 In general, the boundary can be parametrized in terms of the input variables such  
 90 that the cut is set on the parametrization instead of on the variables, i.e.,  $y(\mathbf{x}) = y_{cut}$   
 91 with  $y_{cut}$  being a constant; thus, the acceptance or rejection of an event is based on  
 92 which side of the boundary the event is located. If  $y(\mathbf{x})$ , usually called *test statistic*,  
 93 has functional form, it can be used to determine the probability distribution functions  
 94  $p(y|s)$  and  $p(y|b)$  and then perform a scalar test statistic with a single cut on the scalar  
 95 variable  $y$ .

96 Figure 5.2 illustrates what would be the probability distribution functions under  
 97 the signal and background hypotheses for a scalar test statistic with a cut on the  
 98 classifier  $y$ . Note that the tails of the distributions indicate that some signal events  
 99 fall on the rejection region and some background events fall on the acceptance region;  
 100 therefore, it is convenient to define the *efficiency* with which events of a given type  
 101 are accepted. The signal and background efficiencies are given by



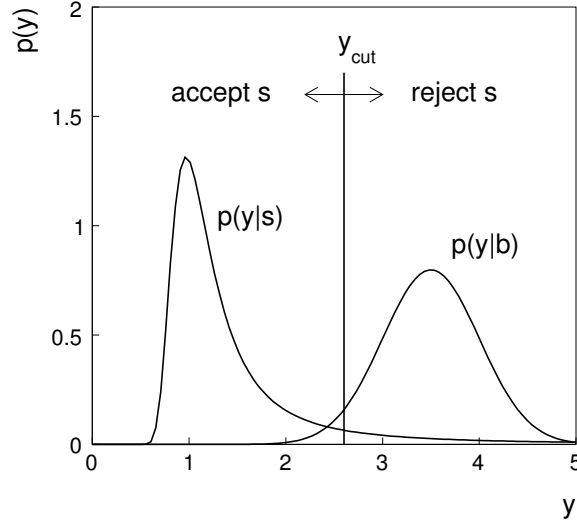


**Figure 5.2:** Distributions of the scalar test statistic  $y(\mathbf{x})$  under the signal and background hypotheses. [126]

$$\varepsilon_s = P(\text{accept event}|s) = \int_A f(\mathbf{x}|s) d\mathbf{x} = \int_{-\infty}^{y_{\text{cut}}} p(y|s) dy, \quad (5.1)$$

$$\varepsilon_b = P(\text{accept event}|b) = \int_A f(\mathbf{x}|b) d\mathbf{x} = \int_{-\infty}^{y_{\text{cut}}} p(y|b) dy, \quad (5.2)$$

102 where  $A$  is the acceptance region. If the background hypothesis is the *null hypothesis*  
 103 ( $H_0$ ), the signal hypothesis would be *alternative hypothesis* ( $H_1$ ); in this context, the  
 104 background efficiency corresponds to the significance level of the test ( $\alpha$ ) and describes  
 105 the misidentification probability, while the signal efficiency corresponds to the power  
 106 of the test ( $1-\beta$ ) and describes the probability of rejecting the background hypothesis  
 107 if the signal hypothesis is true. What is sought in an analysis is to maximize the  
 108 power of the test relative to the significance level, i.e., set a selection with the largest  
 109 possible selection efficiency and the smallest possible misidentification probability.

### 110 5.1.1 Decision trees

111 For this thesis, the implementation of the MVA strategy, described above, is per-  
 112 formed through decision trees by using the TMVA software package [127] included in  
 113 the the ROOT analysis framework [129]. In a simple picture, a decision tree classifies  
 114 events according to their input variables values by setting a cut on each input variable  
 115 and checking which events are on which side of the cut, just as proposed in the MVA  
 116 strategy, but in addition, as a machine learning algorithm, decision trees offer the  
 117 possibility to be trained and then perform the classification efficiently.

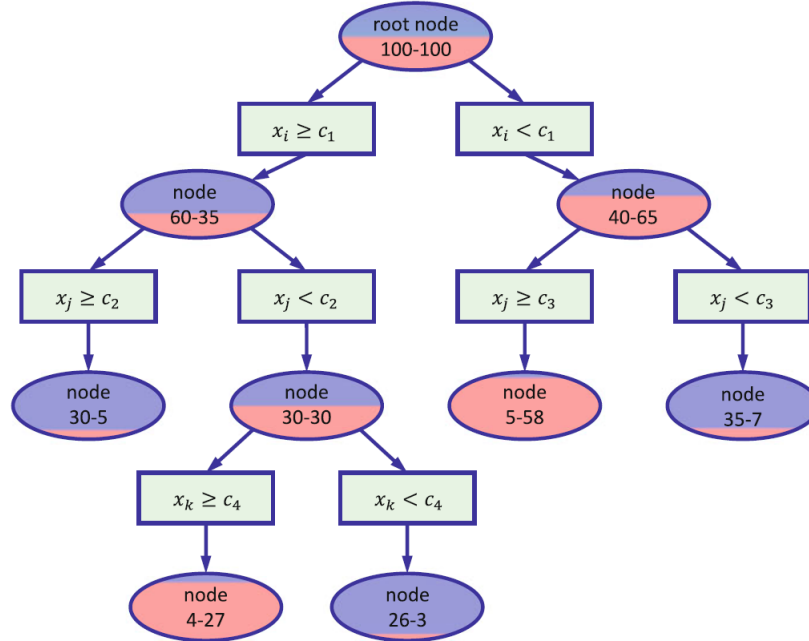


**Figure 5.3:** Example of a decision tree. Each node is fed with a MC sample mixing signal and background events (left-right numbers); nodes colors represent the relative number of signal/background events [128].

118 The training or growing of a decision tree is the process where the rules for clas-  
 119 sifying events are defined; this process is represented in Figure 5.3 and consists of  
 120 several steps:

- 121 • take MC samples of signal and background events and split them into two parts

each; first parts will be used in the decision tree training, while the second parts will be used for testing the final classifier obtained from the training. Each event has associated a set of input variables  $\mathbf{x} = (x_1, \dots, x_n)$  which serve to distinguish between signal and background events. The training sample is taken in at the root *node*.

- pick one variable, say  $x_i$
- pick one value of  $x_i$ , each event has its own value of  $x_i$ , and split the training sample into two subsamples  $B_1$  and  $B_2$ ;  $B_1$  contains events for which  $x_i < c_1$  while  $B_2$  contains the rest of the training events;
- scan all possible values of  $x_i$  and find the splitting value that provides the *best* classification<sup>1</sup>, i.e.,  $B_1$  is mostly made of signal events while  $B_2$  is mostly made of background events.
- It is possible that variables other than the picked one produce a better classification, hence, all the variables have to be evaluated. Pick the next variable, say  $x_j$ , and repeat the scan over its possible values.
- At the end, all the variables and their values will have been scanned, the *best* variable and splitting value will have been identified, say  $x_1, c_1$ , and there will be two nodes fed with the subsamples  $B_1$  and  $B_2$ .

Nodes are further split by repeating the decision process until a given number of final nodes is obtained, nodes are largely dominated by either signal or background events, or nodes have too few events to continue. Final nodes are called *leaves* and they are classified as signal or background leaves according to the class of the majority of events in them. Each *branch* in the tree corresponds to a sequence of cuts.

---

<sup>1</sup> Quality of the classification will be treated in the next paragraph.

145 The quality of the classification at each node is evaluated through a separation  
 146 criteria; there are several of them but the *Gini Index* ( $G$ ) is the one used in the  
 147 decision trees trained for the analysis in this thesis.  $G$  is written in terms of the  
 148 purity ( $P$ ), i.e., the fraction of signal events in the samples after the separation is  
 149 made; it is given by

$$G = P(1 - P) \quad (5.3)$$

150 note that  $P=0.5$  at the root node while  $G=0$  for pure leaves. For a node  $A$  split into  
 151 two nodes  $B_1$  and  $B_2$  the  $G$  gain is

$$\Delta G = G(A) - G(B_1) - G(B_2) \quad (5.4)$$

152 the *best* classification corresponds to that for which the gain of  $G$  is maximized; hence,  
 153 the scanning over all the variables in an event and their values is of great importance.

154 In order to provide a numerical output for the classification, events in a sig-  
 155 nal(background) leaf are assigned an score of 1(-1) each, defining in this way the  
 156 decision tree *classifier/weak learner* as

$$f(\mathbf{x}) = \begin{cases} 1 & \mathbf{x} \text{ in signal region,} \\ -1 & \mathbf{x} \text{ in background region.} \end{cases}$$

157 Figure 5.4 shows an example of the classification of a sample of events, containing  
 158 two variables, performed by a decision tree.

## 159 5.1.2 Boosted decision trees (BDT).

160 Event misclassification occurs when a training event ends up in the wrong leaf, i.e., a  
 161 signal event ends up in a background leaf or a background event ends up in a signal

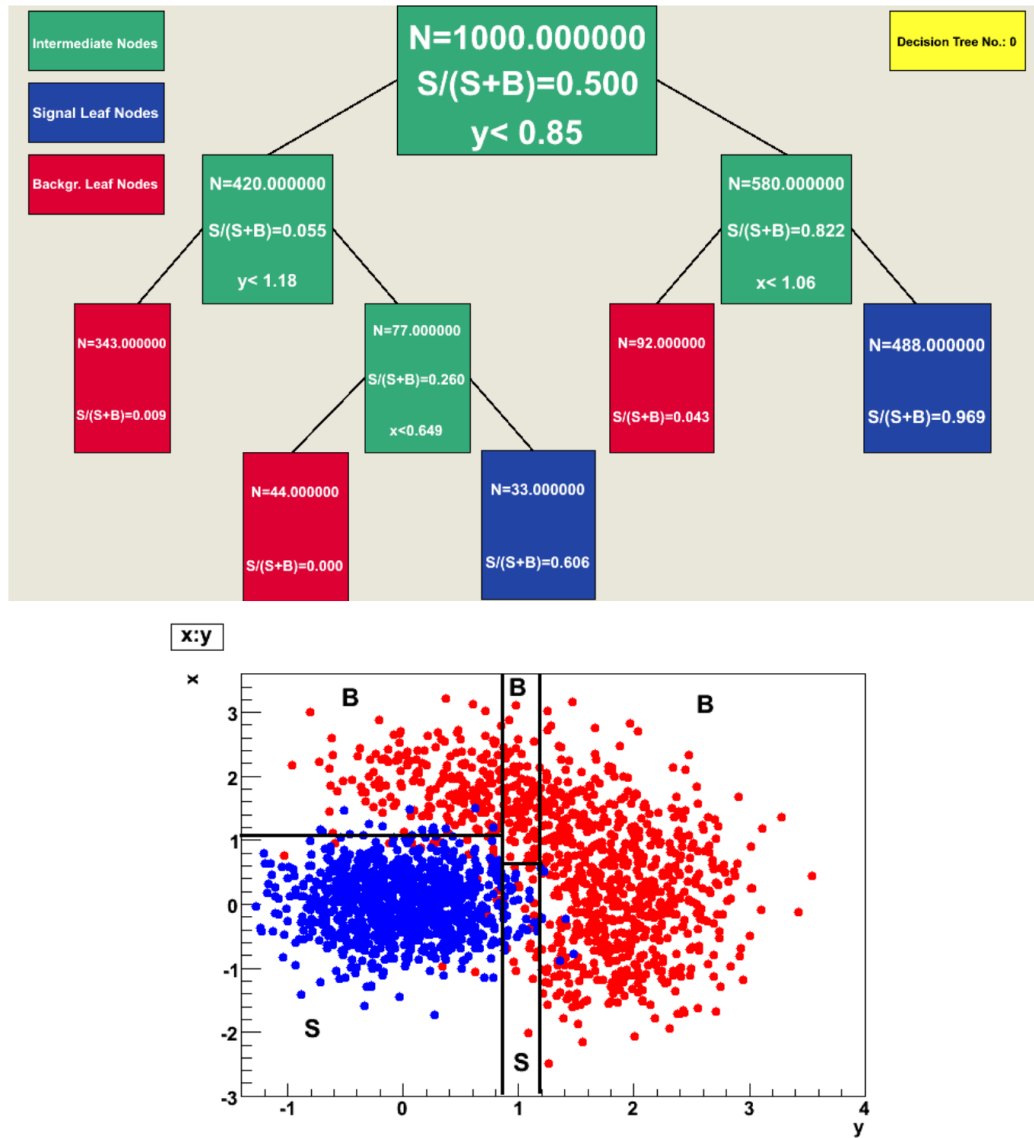


**Figure 5.4:** Example of a decision tree output. Each leaf, blue for signal events and red for background events, is represented by a region in the variables phase space [130].

leaf. A way to correct it is to assign a weight to the misclassified events and train  
a second tree using the reweighted events; the event reweighting is performed by a  
boosting algorithm in such a way that when used in the training of a new decision  
tree the *boosted events* get correctly classified. The process is repeated iteratively  
adding a new tree to the forest and creating a set of classifiers, which are combined

167 to create the next classifier; the final classifier offers more stability<sup>2</sup> and has a smaller  
 168 misclassification rate than any individual ones. The resulting tree collection is known  
 169 as a *boosted decision tree (BDT)*.

170 Thus, purity of the sample is generalized to

$$P = \frac{\sum_s w_s}{\sum_s w_s + \sum_b w_b} \quad (5.5)$$

171 where  $w_s$  and  $w_b$  are the weights of the signal and background events respectively;  
 172 the Gini index is also generalized

$$G = \left( \sum_i^n w_i \right) P(1 - P) \quad (5.6)$$

173 with  $n$  the number of events in the node. The final score of an event, after pass-  
 174 ing through the forest, is calculated as the renormalized sum of all the individual  
 175 (possibly weighted) scores; thus, high(low) score implies that the event is most likely  
 176 signal(background).

177 The boosting procedure, implemented in the *Gradient boosting* algorithm used in  
 178 this thesis, produces a classifier  $F(\mathbf{x})$  which is the weighted sum of the individual  
 179 classifiers obtained after each iteration, i.e.,

$$F(\mathbf{x}) = \sum_{m=1}^M \beta_m f(\mathbf{x}; a_m) \quad (5.7)$$

180 where  $M$  is the number of trees in the forest. The *loss function*  $L(F, y)$  represents the  
 181 deviation between the classifier  $F(\mathbf{x})$  response and the true value  $y$  obtained from the  
 182 training sample (1 for signal events and -1 for background event), according to

---

<sup>2</sup> Decision trees suffer from sensitivity to statistical fluctuations in the training sample which may lead to very different results with an small change in the training samples.

$$L(F, y) = \ln(1 + e^{-2F(\mathbf{x})y}) \quad (5.8)$$

183 thus, the reweighting is employed to ensure the minimization of the loss function; a  
 184 more detailed description of the minimization procedure can be found in Reference  
 185 [131]. The final classifier output is later used as a final discrimination variable, labeled  
 186 as *BDT output/response*.

### 187 5.1.3 Overtraining

188 Decision trees offer the possibility to have as many nodes as wished in order to  
 189 reduce the misclassification to zero (in theory); however, when a classifier is too much  
 190 adjusted to a particular training sample, the classifier's response to a slightly different  
 191 sample may leads to a completely different classification results; this effect is know  
 192 as *overtraining*.

193 An alternative to reduce the overtraining in BDTs consists in pruning the tree  
 194 by removing statistically insignificant nodes after the tree growing is completed but  
 195 this option is not available for BDTs with gradient boosting in the TMVA-toolkit,  
 196 therefore, the overtraining has to be reduced by tuning the algorithm, number of  
 197 nodes, minimum number of events in the leaves, etc. The overtraining can be evalu-  
 198 ated by comparing the responses of the classifier when running over the training and  
 199 test samples.

### 200 5.1.4 Variable ranking

201 BDTs have a couple of particular advantages related to the input variables; on one  
 202 side, they are relatively insensitive to the number of input variables used in the vector  
 203  $\mathbf{x}$ . The ranking of the BDT input variables is determined by counting the number of

times a variable is used to split decision tree nodes; in addition, the separation gain-squared achieved in the splitting and the number of events in the node are accounted by applying a weighting to that number. Thus, those variables with small or no power to separate signal and background events are rarely chosen to split the nodes, i.e., are effectively ignored.

On the other side, variables correlations play an important role for some MVA methods like the Fisher discriminant algorithm in which the first step consist of performing a linear transformation to a phase space where the correlations between variables are removed; in the case of BDT algorithm, correlations do not affect the performance.

### 5.1.5 BDT output example.

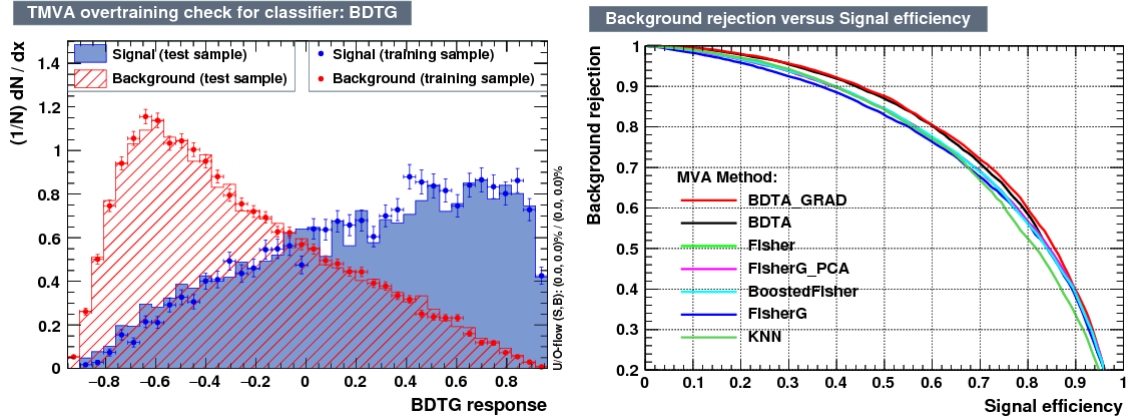


**Figure 5.5:** Left: Output distributions for the gradient boosted decision tree (BDTG) classifier using a sample of signal ( $pp \rightarrow tHq$ ) and background ( $pp \rightarrow t\bar{t}$ ) events. Right: Background rejection vs signal efficiency (ROC curves) for various MVA classifiers running over the same sample used to produce the plot on the left.

Left side of figure 5.5 shows the BDT output distributions for signal ( $pp \rightarrow tHq$ ) and background ( $pp \rightarrow t\bar{t}$ ) events; this plot is the equivalent to the one showed in Figure 5.2. A forest with 800 trees, maximum depth per tree = 3, and gradient



218 boosting have been used as training parameters. The BDTG classifier offers a good  
 219 separation power; while there is a small overtraining in the signal distribution, the  
 220 background distribution seems to be well predicted which might indicate that the  
 221 sample is composed of more background than signal events.

222 Right side of figure 5.5 shows the background rejection vs signal efficiency curves  
 223 for several combinations of MVA classifiers-boosting algorithms; these curves are  
 224 known as ROC curves and give an indication of the performance of the classifier. The  
 225 best performance is achieved with the BDTG classifier (BDTA\_GRAD).

## 226 5.2 Statistical inference.

227 Once events are classified, the next step consists in finding the parameters that define  
 228 the likelihood functions  $f(\mathbf{x}|s), f(\mathbf{x}|b)$  for signal and background events respectively.  
 229 In general, likelihood functions depend not only on the measurements but also on  
 230 parameters ( $\theta_m$ ) that define their shapes; the process of estimating these *unknown*  
 231 *parameters* and their uncertainties from the experimental data is called *inference*.

### 232 5.2.1 Nuisance parameters.

233 The unknown parameter vector  $\boldsymbol{\theta}$  is made of two types of parameters: on one side,  
 234 those parameters that provide information about the physical observables of interest  
 235 for the experiment or *parameters of interest*. On the other side, the *nuisance param-*  
 236 *eters* that are not of direct interest for the experiment but that need to be included in  
 237 the analysis in order to achieve a satisfactory description of the data; they represent  
 238 effects of the detector response like the finite resolutions of the detection systems,  
 239 miscalibrations, and in general any source of uncertainty introduced in the analysis.

240 Nuisance parameters can be estimated from experimental data; for instance, data  
 241 samples from a test beam are usually employed for calibration purposes. In cases  
 242 where experimental samples are not available, the estimation of nuisance parameters  
 243 makes use of dedicated simulation programs to provide the required samples.

244 The estimation of the unknown parameters involves certain deviation from their  
 245 true values, hence, the measurement of the nuisance parameter is written in terms  
 246 of an estimated value, also called central value,  $\hat{\theta}$  and its uncertainty  $\delta\theta$  using the  
 247 notation

$$\theta = \hat{\theta} \pm \delta\theta \quad (5.9)$$

248 where the interval  $[\hat{\theta} - \delta\theta, \hat{\theta} + \delta\theta]$  is called *confidence interval*; it is usually interpreted,  
 249 in the limit of infinite number of experiments, as the interval where the true value  
 250 of the unknown parameter  $\theta$  is contained with a probability of 0.6827 (if no other  
 251 convention is stated); this interval represents the area under a Gaussian distribution  
 252 in the interval  $\pm 1\sigma$ .

253 The uncertainties associated to nuisance parameters produce *systematic uncer-*  
 254 *tainties* in the final measurement, while the uncertainties related only to fluctuations  
 255 in data and that affect the determination of parameters of interest produce *statistical*  
 256 *uncertainties*.

## 257 5.2.2 Maximum likelihood estimation method

258 The estimation of the unknown parameters that are in best agreement with the ob-  
 259 served data is performed through a function of the data sample that return the  
 260 estimate of those parameters; that function is called an *estimator*. Estimators are  
 261 usually constructed using mathematical expressions encoded in algorithms.

262 In this thesis, the estimator used is the likelihood function  $f(\mathbf{x}|\boldsymbol{\theta})$ <sup>3</sup> which depends  
 263 on a set of measured variables  $\mathbf{x}$  and a set of unknown parameters  $\boldsymbol{\theta}$ . The likelihood  
 264 function for N events in a sample is the combination of all the individual likelihoods  
 265 functions, i.e.,

$$L(\boldsymbol{\theta}) = \prod_{i=1}^N f(\mathbf{x}^i|\boldsymbol{\theta}) = \prod_{i=1}^N f(x_1^i, \dots, x_n^i; \theta_1, \dots, \theta_m) \quad (5.10)$$

266 and the estimation method used is the *Maximum Likelihood Estimation* method  
 267 (MLE); it is based on the combined likelihood function defined by eqn. 5.10 and  
 268 the procedure seeks for the parameter set that corresponds to the maximum value of  
 269 the combined likelihood function, i.e., the *maximum likelihood estimator* of the un-  
 270 known parameter vector  $\boldsymbol{\theta}$  is the function that produces the vector of *best estimators*  
 271  $\hat{\boldsymbol{\theta}}$  for which the likelihood function  $L(\boldsymbol{\theta})$  evaluated at the measured  $\mathbf{x}$  is maximum.

272 Usually, the logarithm of the likelihood function is used in numerical algorithm  
 273 implementations in order to avoid underflow the numerical precision of the computers  
 274 due to the product of low likelihoods. In addition, it is common to minimize the  
 275 negative logarithm of the likelihood function, therefore, the negative log-likelihood  
 276 function is

$$F(\boldsymbol{\theta}) = -\ln L(\boldsymbol{\theta}) = -\sum_{i=1}^N f(\mathbf{x}^i|\boldsymbol{\theta}). \quad (5.11)$$

277 The minimization process is performed by the software MINUIT [132] imple-  
 278 mented in the ROOT analysis framework. In case of data samples with large number  
 279 of measurements, the computational resources necessary to calculate the likelihood  
 280 function are too big; therefore, the parameter estimation is performed using binned  
 281 distributions of the variables of interest for which the *binned likelihood function* is

---

<sup>3</sup> analogue to the likely functions described in previous sections

282 given by

$$L(\mathbf{x}|r, \boldsymbol{\theta}) = \prod_{i=1} \frac{(r \cdot s_i(\boldsymbol{\theta}) + b_i(\boldsymbol{\theta}))^{n_i}}{n_i!} e^{-r \cdot s_i(\boldsymbol{\theta}) - b_i(\boldsymbol{\theta})} \prod_{j=1} \frac{1}{\sqrt{2\pi}\sigma_{\theta_j}^2} e^{-(\theta_j - \theta_{0,j})^2 / 2\sigma_{\theta_j}^2}, \quad (5.12)$$

283 with  $s_i$  and  $b_i$  the expected number of signal and background yields for the bin  $i$ ,  $n_i$   
 284 is the observed number of events in the bin  $i$  and  $r = \sigma/\sigma_{SM}$  is the signal strength.  
 285 Note that the number of entries per bin follows a Poisson distribution. The effect  
 286 of the nuisance parameters have been included in the likelihood function through  
 287 the multiplication by a Gaussian distribution that models the nuisance. The three  
 288 parameters,  $r$ ,  $s_i$  and  $b_i$  are jointly fitted to estimate the value of  $r$ .

### 289 5.3 Upper limits

290 In this analysis, two hypotheses are considered; the background only hypothesis  
 291 ( $H_0(b)$ ) and the signal plus background hypothesis ( $H_1(s+b)$ ), i.e., the sample of  
 292 events is composed of background only events ( $r=0$ ) or it is a mixture of signal plus  
 293 background events ( $r=1$ ). The exclusion of one hypothesis against the other means  
 294 that the observed data sample better agrees with  $H_0$  or rather with  $H_1$ . In order  
 295 to discriminate these hypotheses, a test statistic is constructed on the basis of the  
 296 likelihood function evaluated for each of the hypothesis.

297 The *Neyman-Pearson* lemma [133] states that the test statistic that provide the  
 298 maximum power for  $H_1$  for a given significance level (background misidentification  
 299 probability  $\alpha$ ), is given by the ratio of the likelihood functions  $L(\mathbf{x}|H_1)$  and  $L(\mathbf{x}|H_0)$ ;  
 300 however, in order to use that definition it is necessary to know the true likelihood  
 301 functions, which in practice is not always possible. Approximate functions obtained  
 302 by numerical methods, like the BDT method described above, have to be used, so

303 that the *profile likelihood* test statistic is defined by

$$\lambda(\mathbf{r}) = \frac{L(\mathbf{x}|r, \hat{\boldsymbol{\theta}}(r))}{L(\mathbf{x}|\hat{r}, \hat{\boldsymbol{\theta}})}, \quad (5.13)$$

304 where,  $\hat{r}$  and  $\hat{\boldsymbol{\theta}}$  maximize the likelihood function, and  $\hat{\boldsymbol{\theta}}$  maximize the likelihood  
 305 function for a given value of the signal strength modifier  $r$ . In practice, the test  
 306 statistic  $t_r$

$$t_r = -2\ln\lambda(r) \quad (5.14)$$

307 is used to evaluate the presence of signal in the sample, since the minimum of  $t_r$  at  
 308  $r = \hat{r}$  suggest the presence of signal with signal strength  $\hat{r}$ . The uncertainty interval  
 309 for  $r$  is determined by the values of  $r$  for which  $t_r = 1$ .

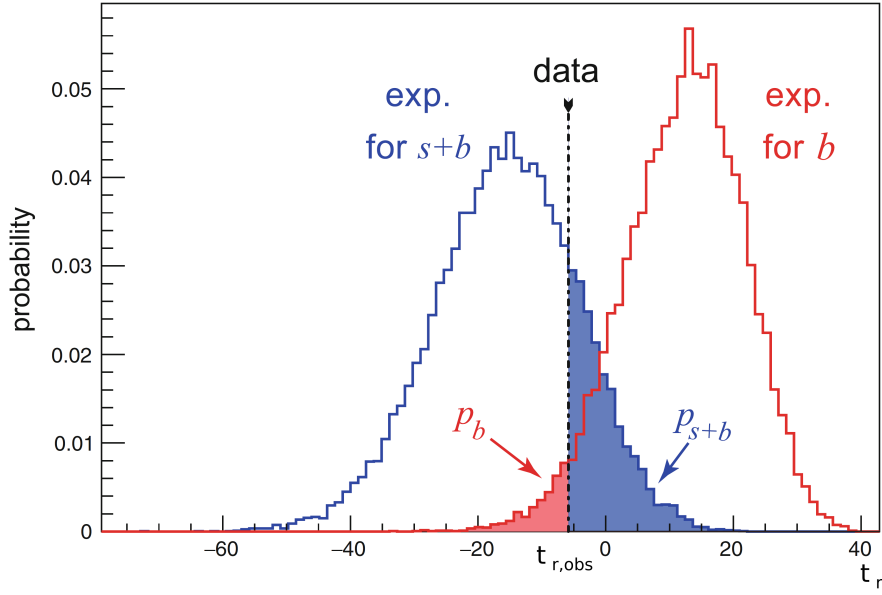


**Figure 5.6:**  $t_r$  p.d.f. from MC pseudo experiments assuming  $H_0$  (red) and  $H_1$  (blue). The black dashed line shows the value of the test statistic as measured from data. Adapted from Reference [128].

310 The expected probability density function (p.d.f)  $f(t_r|r, \boldsymbol{\theta})$  of the test statistic  $t_r$   
 311 can be obtained numerically by generating MC pseudo-experiments assuming each  $H_0$

and  $H_1$  as shown in Figure 5.6. The probability that  $t_r$  takes a value equal or greater than the observed value ( $t_{r,obs}$ ) when a signal with a signal modifier  $r$  is present in the data sample, is called *p-value* of the observation; it can be calculated using

$$p_r = \int_{t_{r,obs}}^{\infty} f(t'_r|r, \boldsymbol{\theta}) dt'_r, \quad (5.15)$$

thus,  $p_r < 0.05$  means that, for that particular value of  $r$ ,  $H_1$  could be excluded at 95% Confidence Level (CL). The corresponding background-only p-value is given by

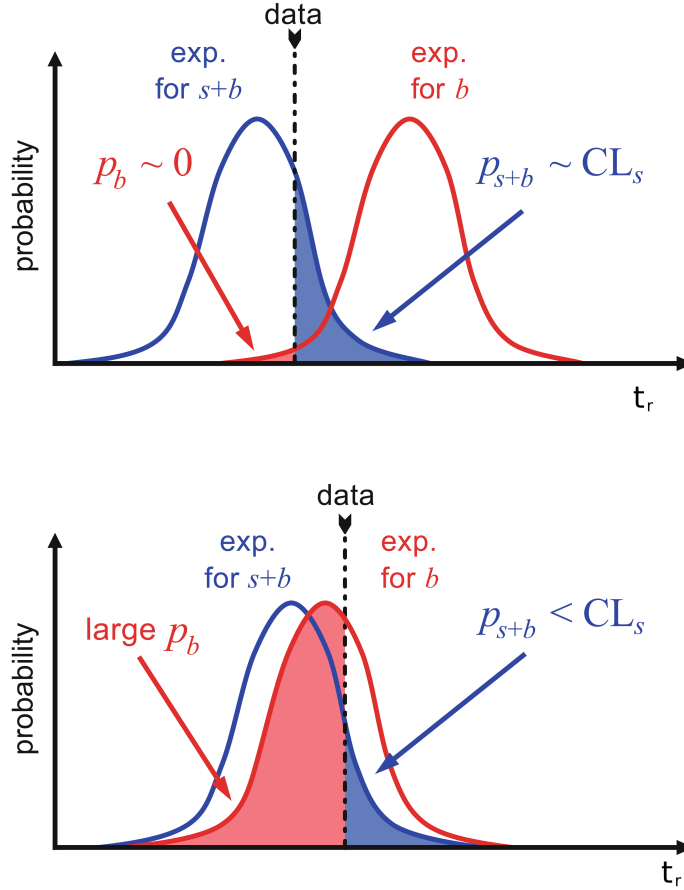


**Figure 5.7:**  $CL_s$  limit illustration. When the test statistic p.d.f. for the two hypotheses  $H_0$  and  $H_1$  are well separated (top) and when they are largely overlapped (bottom). Adapted from Reference [128].

$$1 - p_b = \int_{t_{r,obs}}^{\infty} f(t'_r|0, \boldsymbol{\theta}) dt'_r, \quad (5.16)$$

317 If the  $t_r$  p.d.f. for both hypotheses are well separated, as shown in the top side of  
 318 Figure 5.7, the experiment is sensitive to the presence of signal in the sample. If the  
 319 signal presence is small, both p.d.f. will be largely overlapped and either the signal  
 320 hypothesis could be rejected with not enough justification because experiment is not  
 321 sensitive to the signal or a fluctuation of the background could be misinterpreted as  
 322 presence of signal with the corresponding rejection of the background-only hypothesis.  
 323 These issues are corrected by using the modified p-value [135]

$$p'_r = \frac{p_r}{1 - p_b} \equiv CL_s \quad (5.17)$$

324 the upper limit of the parameter of interest  $r^{up}$  if determined by scanning over  $r$   
 325 and find the value for which  $p'^{up}_r = 0.05$ . The expected upper limit can be calculated  
 326 using pseudo-experiments based on the background-only hypothesis and obtaining a  
 327 distribution for  $r^{up}_{ps}$ ; the median of that distribution corresponds to the expected upper  
 328 limit, while the  $\pm 1\sigma$  and  $\pm 2\sigma$  deviations correspond to the values of the distribution  
 329 that defines the 68% and 95% of the area under the distribution centered in the  
 330 median. It is usual to present all the information about the expected and observed  
 331 limits in the so-called *Brazilian-flag plot* as the one showed in Figure 5.8.

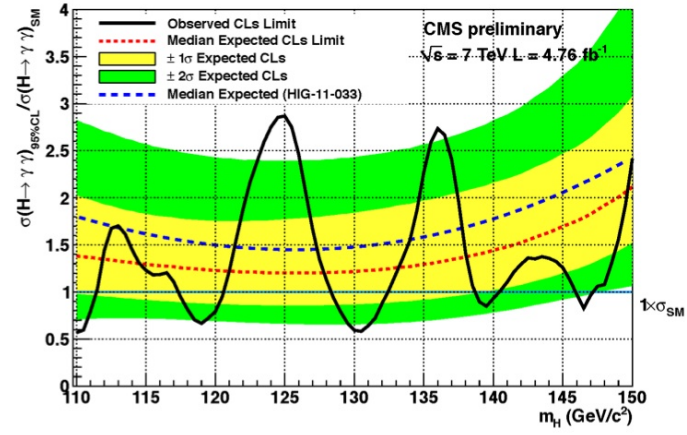


**Figure 5.8:** Brazilian flag plot of CMS experiment limits for Higgs boson decaying to photons [136].



## References

- 333 [1] J. Schwinger. “Quantum Electrodynamics. I. A Covariant Formulation”. Phys-  
 334 ical Review. 74 (10): 1439-61, (1948). [https://doi.org/10.1103/PhysRev.](https://doi.org/10.1103/PhysRev.74.1439)  
 335 [74.1439](https://doi.org/10.1103/PhysRev.74.1439)
- 336 [2] R. P. Feynman. “Space-Time Approach to Quantum Electrodynamics”. Physical  
 337 Review. 76 (6): 769-89, (1949). <https://doi.org/10.1103/PhysRev.76.769>
- 338 [3] S. Tomonaga. “On a Relativistically Invariant Formulation of the Quantum  
 339 Theory of Wave Fields”. Progress of Theoretical Physics. 1 (2): 27-42, (1946).  
 340 <https://doi.org/10.1143/PTP.1.27>
- 341 [4] D.J. Griffiths, “Introduction to electrodynamics”. 4th ed. Pearson, (2013).
- 342 [5] F. Mandl, G. Shaw. “Quantum field theory.” Chichester, Wiley (2009).
- 343 [6] F. Halzen, and A.D. Martin, “Quarks and leptons: An introductory course in  
 344 modern particle physics”. New York: Wiley, (1984) .
- 345 [7] File: Standard\_Model\_of\_Elementary\_Particle\_dark.svg. (2017, June 12)  
 346 Wikimedia Commons, the free media repository. Retrieved November 27, 2017  
 347 from [https://www.collegiate-advanced-electricity.com/single-post/](https://www.collegiate-advanced-electricity.com/single-post/2017/04/10/The-Standard-Model-of-Particle-Physics)  
 348 [2017/04/10/The-Standard-Model-of-Particle-Physics](https://www.collegiate-advanced-electricity.com/single-post/2017/04/10/The-Standard-Model-of-Particle-Physics).

- 349 [8] E. Noether, “Invariante Variationsprobleme”, Nachrichten von der Gesellschaft  
350 der Wissenschaften zu Göttingen, mathematisch-physikalische Klasse, vol. 1918,  
351 pp. 235-257, (1918).
- 352 [9] C. Patrignani et al. (Particle Data Group), Chin. Phys. C, 40, 100001 (2016)  
353 and 2017 update.
- 354 [10] M. Goldhaber, L. Grodzins, A.W. Sunyar “Helicity of Neutrinos”, Phys. Rev.  
355 109, 1015 (1958).
- 356 [11] Palanque-Delabrouille N et al. “Neutrino masses and cosmology with Lyman-  
357 alpha forest power spectrum”, JCAP 11 011 (2015).
- 358 [12] M. Gell-Mann. “A Schematic Model of Baryons and Mesons”. Physics Letters.  
359 8 (3): 214-215 (1964).
- 360 [13] G. Zweig. “An SU(3) Model for Strong Interaction Symmetry and its Breaking”  
361 (PDF). CERN Report No.8182/TH.401 (1964).
- 362 [14] G. Zweig. “An SU(3) Model for Strong Interaction Symmetry and its Breaking:  
363 II” (PDF). CERN Report No.8419/TH.412(1964).
- 364 [15] M. Gell-Mann. “The Interpretation of the New Particles as Displaced Charged  
365 Multiplets”. Il Nuovo Cimento 4: 848. (1956).
- 366 [16] T. Nakano, K, Nishijima. “Charge Independence for V-particles”. Progress of  
367 Theoretical Physics 10 (5): 581-582. (1953).
- 368 [17] N. Cabibbo, “Unitary symmetry and leptonic decays” Physical Review Letters,  
369 vol. 10, no. 12, p. 531, (1963).

- [18] M.Kobayashi, T.Maskawa, “CP-violation in the renormalizable theory of weak interaction,” Progress of Theoretical Physics, vol. 49, no. 2, pp. 652-657, (1973).
- [19] File: Weak Decay (flipped).svg. (2017, June 12). Wikimedia Commons, the free media repository. Retrieved November 27, 2017 from [https://commons.wikimedia.org/w/index.php?title=File:Weak\\_Decay\\_\(flipped\)\.svg&oldid=247498592](https://commons.wikimedia.org/w/index.php?title=File:Weak_Decay_(flipped)\.svg&oldid=247498592).
- [20] Georgia Tech University. Coupling Constants for the Fundamental Forces(2005). Retrieved January 10, 2018, from <http://hyperphysics.phy-astr.gsu.edu/hbase/Forces/couple.html#c2>
- [21] M. Strassler. (May 31, 2013).The Strengths of the Known Forces. Retrieved January 10, 2018, from <https://profmattstrassler.com/articles-and-posts/particle-physics-basics/the-known-forces-of-nature/the-strength-of-the-known-forces/>
- [22] S.L. Glashow. “Partial symmetries of weak interactions”, Nucl. Phys. 22 579-588, (1961).
- [23] A. Salam, J.C. Ward. “Electromagnetic and weak interactions”, Physics Letters 13 168-171, (1964).
- [24] S. Weinberg, “A model of leptons”, Physical Review Letters, vol. 19, no. 21, p. 1264, (1967).
- [25] M. Peskin, D. Schroeder, “An introduction to quantum field theory”. Perseus Books Publishing L.L.C., (1995).
- [26] A. Pich. “The Standard Model of Electroweak Interactions” <https://arxiv.org/abs/1201.0537>

- 393 [27] G. Arnison et al. (UA1 Collaboration), Phys. Lett. B 122, 103 (1983).
- 394 [28] M. Banner et al. (UA2 Collaboration), Phys. Lett. B 122, 476 (1983).
- 395 [29] G. Arnison et al. (UA1 Collaboration), Phys. Lett. B 126, 398 (1983).
- 396 [30] P. Bagnaia et al. (UA2 Collaboration), Phys. Lett. B 129, 130 (1983).
- 397 [31] F.Bellaiche. (2012, 2 September). “What’s this Higgs boson anyway?”. Retrieved  
398 from: <https://www.quantum-bits.org/?p=233>
- 399 [32] M. Endres et al. Nature 487, 454-458 (2012) doi:10.1038/nature11255
- 400 [33] F. Englert, R. Brout. “Broken Symmetry and the Mass of Gauge  
401 Vector Mesons”. Physical Review Letters. 13 (9): 321-23.(1964)  
402 doi:10.1103/PhysRevLett.13.321
- 403 [34] P.Higgs. “Broken Symmetries and the Masses of Gauge Bosons”. Physical Re-  
404 view Letters. 13 (16): 508-509,(1964). doi:10.1103/PhysRevLett.13.508.
- 405 [35] G.Guralnik, C.R. Hagen and T.W.B. Kibble. “Global Conservation Laws  
406 and Massless Particles”. Physical Review Letters. 13 (20): 585-587, (1964).  
407 doi:10.1103/PhysRevLett.13.585.
- 408 [36] CMS collaboration. “Observation of a new boson at a mass of 125 GeV with  
409 the CMS experiment at the LHC”. Physics Letters B. 716 (1): 30-61 (2012).  
410 arXiv:1207.7235. doi:10.1016/j.physletb.2012.08.021
- 411 [37] ATLAS collaboration. “Observation of a New Particle in the Search for the Stan-  
412 dard Model Higgs Boson with the ATLAS Detector at the LHC”. Physics Letters  
413 B. 716 (1): 1-29 (2012). arXiv:1207.7214. doi:10.1016/j.physletb.2012.08.020.

- 414 [38] ATLAS collaboration; CMS collaboration (26 March 2015). “Combined Mea-  
 415 surement of the Higgs Boson Mass in pp Collisions at  $\sqrt{s}=7$  and 8 TeV with  
 416 the ATLAS and CMS Experiments”. Physical Review Letters. 114 (19): 191803.  
 417 arXiv:1503.07589. doi:10.1103/PhysRevLett.114.191803.
- 418 [39] LHC InternationalMasterclasses“When protons collide”. Retrieved from [http:](http://atlas.physicsmasterclasses.org/en/zpath_protoncollisions.htm)  
 419 [//atlas.physicsmasterclasses.org/en/zpath\\_protoncollisions.htm](http://atlas.physicsmasterclasses.org/en/zpath_protoncollisions.htm)
- 420 [40] CMS Collaboration, “SM Higgs Branching Ratios and Total Decay Widths (up-  
 421 date in CERN Report4 2016)”. [https://twiki.cern.ch/twiki/bin/view/](https://twiki.cern.ch/twiki/bin/view/LHCPhysics/CERNYellowReportPageBR)  
 422 [LHCPhysics/CERNYellowReportPageBR](https://twiki.cern.ch/twiki/bin/view/LHCPhysics/CERNYellowReportPageBR) , last accessed on 17.12.2017.
- 423 [41] R.Grant V. “Determination of Higgs branching ratios in  $H \rightarrow W^+W^- \rightarrow l\nu jj$   
 424 and  $H \rightarrow ZZ \rightarrow l^+l^- jj$  channels”. Physics Department, University of Ten-  
 425 nessee (Dated: October 31, 2012). Retrieved from [http://aesop.phys.utk.](http://aesop.phys.utk.edu/ph611/2012/projects/Riley.pdf)  
 426 [edu/ph611/2012/projects/Riley.pdf](http://aesop.phys.utk.edu/ph611/2012/projects/Riley.pdf)
- 427 [42] LHC Higgs Cross Section Working Group, Denner, A., Heinemeyer, S. et al.  
 428 “Standard model Higgs-boson branching ratios with uncertainties”. Eur. Phys.  
 429 J. C (2011) 71: 1753. <https://doi.org/10.1140/epjc/s10052-011-1753-8>
- 430 [43] D. de Florian et al., LHC Higgs Cross Section Working Group,  
 431 CERNâ€š2017â€š002-M, arXiv:1610.07922[hep-ph] (2016).
- 432 [44] ATLAS and CMS Collaborations, “Measurements of the Higgs boson produc-  
 433 tion and decay rates and constraints on its couplings from a combined ATLAS  
 434 and CMS analysis of the LHC pp collision data at  $\sqrt{s} = 7$  and 8 TeV,” (2016).  
 435 CERN-EP-2016-100, ATLAS-HIGG-2015-07, CMS-HIG-15-002.

- [45] J. A. Aguilar-Saavedra, R. Benbrik, S. Heinemeyer, and M. Perez-Victoria,  
 “Handbook of vector-like quarks: Mixing and single production”, Phys. Rev. D  
 88 (2013) 094010, doi:10.1103/PhysRevD.88.094010, arXiv:1306.0572.
- [46] A. Greljo, J. F. Kamenik, and J. Kopp, “Disentangling flavor vio-  
 lation in the top-Higgs sector at the LHC”, JHEP 07 (2014) 046,  
 doi:10.1007/JHEP07(2014)046, arXiv:1404.1278.
- [47] F. Demartin, F. Maltoni, K. Mawatari, and M. Zaro, “Higgs production in  
 association with a single top quark at the LHC,” European Physical Journal C,  
 vol. 75, p. 267, (2015). doi:10.1140/epj c/s10052-015-3475-9, arXiv:1504.00611.
- [48] F. Demartin, B. Maier, F. Maltoni, K. Mawatari, and M. Zaro, “tWH associated  
 production at the LHC”, European Physical Journal C, vol. 77, p. 34, (2017).  
 arXiv:1607.05862
- [49] F. Maltoni, K. Paul, T. Stelzer, and S. Willenbrock, “Associated production  
 of Higgs and single top at hadron colliders”, Phys.Rev. D64 (2001) 094023,  
 [hep-ph/0106293].
- [50] S. Biswas, E. Gabrielli, F. Margaroli, and B. Mele, “Direct constraints on the  
 top-Higgs coupling from the 8 TeV LHC data,” Journal of High Energy Physics,  
 vol. 07, p. 073, (2013).
- [51] M. Farina, C. Grojean, F. Maltoni, E. Salvioni, and A. Thamm, “Lifting de-  
 generacies in Higgs couplings using single top production in association with a  
 Higgs boson,” Journal of High Energy Physics, vol. 05, p. 022, (2013).
- [52] T.M. Tait and C.-P. Yuan, “Single top quark production as a window to physics  
 beyond the standard model”, Phys. Rev. D 63 (2000) 014018 [hep-ph/0007298].

- 459 [53] CMS Collaboration, “Modelling of the single top-quark production in associa-  
 460 tion with the Higgs boson at 13 TeV.” [https://twiki.cern.ch/twiki/bin/](https://twiki.cern.ch/twiki/bin/viewauth/CMS/SingleTopHiggsGeneration13TeV)  
 461 [viewauth/CMS/SingleTopHiggsGeneration13TeV](https://twiki.cern.ch/twiki/bin/viewauth/CMS/SingleTopHiggsGeneration13TeV), last accessed on 16.01.2018.
- 462 [54] CMS Collaboration, “SM Higgs production cross sections at  $\sqrt{s} =$   
 463 13 TeV.” [https://twiki.cern.ch/twiki/bin/view/LHCPhysics/](https://twiki.cern.ch/twiki/bin/view/LHCPhysics/CERNYellowReportPageAt13TeV)  
 464 [CERNYellowReportPageAt13TeV](https://twiki.cern.ch/twiki/bin/view/LHCPhysics/CERNYellowReportPageAt13TeV), last accessed on 16.01.2018.
- 465 [55] S. Dawson, The effective W approximation, Nucl. Phys. B 249 (1985) 42.
- 466 [56] S. Biswas, E. Gabrielli and B. Mele, JHEP 1301 (2013) 088 [arXiv:1211.0499  
 467 [hep-ph]].
- 468 [57] LHC Higgs Cross Section Working Group, “Handbook of LHC Higgs Cross  
 469 Sections: 4.Deciphering the Nature of the Higgs Sector”, arXiv:1610.07922.
- 470 [58] J. Ellis, D. S. Hwang, K. Sakurai, and M. Takeuchi, “Disentangling Higgs-Top  
 471 Couplings in Associated Production”, JHEP 1404 (2014) 004, [arXiv:1312.5736].
- 472 [59] CMS Collaboration, V. Khachatryan et al., “Precise determination of the mass  
 473 of the Higgs boson and tests of compatibility of its couplings with the standard  
 474 model predictions using proton collisions at 7 and 8 TeV,” arXiv:1412.8662.
- 475 [60] ATLAS Collaboration, G. Aad et al., “Updated coupling measurements of the  
 476 Higgs boson with the ATLAS detector using up to 25 fb<sup>-1</sup> of proton-proton  
 477 collision data”, ATLAS-CONF-2014-009.
- 478 [61] File:Cern-accelerator-complex.svg. Wikimedia Commons, the free media repos-  
 479 itory. Retrieved January, 2018 from [https://commons.wikimedia.org/wiki/](https://commons.wikimedia.org/wiki/File:Cern-accelerator-complex.svg)  
 480 [File:Cern-accelerator-complex.svg](https://commons.wikimedia.org/wiki/File:Cern-accelerator-complex.svg)

- 481 [62] J.L. Caron , “Layout of the LEP tunnel including future LHC infrastructures.”,  
482 (Nov, 1993). A C Collection. Legacy of AC. Pictures from 1992 to 2002. Re-  
483 trieved from <https://cds.cern.ch/record/841542>
- 484 [63] M. Vretenar, “The radio-frequency quadrupole”. CERN Yellow Report CERN-  
485 2013-001, pp.207-223 DOI:10.5170/CERN-2013-001.207. arXiv:1303.6762
- 486 [64] L.Evans. P. Bryant (editors). “LHC Machine”. JINST 3 S08001 (2008).
- 487 [65] CERN Photographic Service:“Radio-frequency quadrupole, RFQ-1”, March  
488 1983, CERN-AC-8303511. Retrieved from [https://cds.cern.ch/record/](https://cds.cern.ch/record/615852)  
489 615852.
- 490 [66] CERN Photographic Service “Animation of CERN’s accelerator network”, 14  
491 October 2013. DOI: 10.17181/cds.1610170 Retrieved from [https://videos.](https://videos.cern.ch/record/1610170)  
492 [cern.ch/record/1610170](https://videos.cern.ch/record/1610170)
- 493 [67] C.Sutton. “Particle accelerator”.Encyclopedia Britannica. July 17,  
494 2013. Retrieved from [https://www.britannica.com/technology/](https://www.britannica.com/technology/particle-accelerator)  
495 [particle-accelerator.](https://www.britannica.com/technology/particle-accelerator)
- 496 [68] L.Guiraud. “Installation of LHC cavity in vacuum tank.”. July 27 2000. CERN-  
497 AC-0007016. Retrieved from <https://cds.cern.ch/record/41567>.
- 498 [69] J.L. Caron, “Magnetic field induced by the LHC dipole’s superconducting coils”.  
499 March 1998. AC Collection. Legacy of AC. Pictures from 1992 to 2002. LHC-  
500 PHO-1998-325. Retrieved from <https://cds.cern.ch/record/841511>.
- 501 [70] AC Team. “Diagram of an LHC dipole magnet”. June 1999. CERN-DI-9906025  
502 retrieved from <https://cds.cern.ch/record/40524>.



- 503 [71] CMS Collaboration “Public CMS Luminosity Information”. [https://twiki.cern.ch/twiki/bin/view/CMSPublic/LumiPublicResults#2016\\\_proton\\\_proton\\\_13\\\_TeV\\\_collis](https://twiki.cern.ch/twiki/bin/view/CMSPublic/LumiPublicResults#2016\_proton\_proton\_13\_TeV\_collis), last accessed 24.01.2018
- 504
- 505
- 506 [72] J.L. Caron. “LHC Layout” AC Collection. Legacy of AC. Pictures from 1992
- 507 to 2002. September 1997, LHC-PHO-1997-060. Retrieved from <https://cds.cern.ch/record/841573>.
- 508
- 509 [73] J.A. Coarasa. “The CMS Online Cluster:Setup, Operation and Maintenance
- 510 of an Evolving Cluster”. ISGC 2012, 26 February - 2 March 2012, Academia
- 511 Sinica, Taipei, Taiwan.
- 512 [74] CMS Collaboration. “The CMS experiment at the CERN LHC” JINST 3 S08004
- 513 (2008).
- 514 [75] CMS Collaboration. “CMS detector drawings 2012” CMS-PHO-GEN-2012-002.
- 515 Retrieved from <http://cds.cern.ch/record/1433717>.
- 516 [76] Davis, Siona Ruth. “Interactive Slice of the CMS detector”, Aug. 2016,
- 517 CMS-OUTREACH-2016-027, retrieved from <https://cds.cern.ch/record/2205172>
- 518
- 519 [77] R. Breedon. “View through the CMS detector during the cooldown of the
- 520 solenoid on February 2006. CMS Collection”, February 2006, CMS-PHO-
- 521 OREACH-2005-004, Retrieved from <https://cds.cern.ch/record/930094>.
- 522 [78] Halyo, V. and LeGresley, P. and Lujan, P. “Massively Parallel Computing and
- 523 the Search for Jets and Black Holes at the LHC”, Nucl.Instrum.Meth. A744
- 524 (2014) 54-60, DOI: 10.1016/j.nima.2014.01.038”

- 525 [79] A. Dominguez et. al. “CMS Technical Design Report for the Pixel Detector  
526 Upgrade”, CERN-LHCC-2012-016. CMS-TDR-11.
- 527 [80] CMS Collaboration. “Description and performance of track and primary-vertex  
528 reconstruction with the CMS tracker,” Journal of Instrumentation, vol. 9, no.  
529 10, p. P10009,(2014).
- 530 [81] CMS Collaboration and M. Brice. “Images of the CMS Tracker Inner Bar-  
531 rel”, November 2008, CMS-PHO-TRACKER-2008-002. Retrieved from <https://cds.cern.ch/record/1431467>.  
532
- 533 [82] M. Weber. “The CMS tracker”. 6th international conference on hyperons, charm  
534 and beauty hadrons Chicago, June 28-July 3 2004.
- 535 [83] CMS Collaboration. “Projected Performance of an Upgraded CMS Detector at  
536 the LHC and HL-LHC: Contribution to the Snowmass Process”. Jul 26, 2013.  
537 arXiv:1307.7135
- 538 [84] L. Veillet. “End assembly of HB with EB rails and rotation inside SX ”,Jan-  
539 uary 2002. CMS-PHO-HCAL-2002-002. Retrieved from <https://cds.cern.ch/record/42594>.  
540
- 541 [85] J. Puerta-Pelayo.“First DT+RPC chambers installation round in the UX5 cav-  
542 ern.”. January 2007, CMS-PHO-OREACH-2007-001. Retrieved from <https://cds.cern.ch/record/1019185>  
543
- 544 [86] X. Cid Vidal and R. Cid Manzano. “CMS Global Muon Trigger” web site:  
545 Taking a closer look at LHC. Retrieved from [https://www.lhc-closer.es/taking\\_a\\_closer\\_look\\_at\\_lhc/0.lhc\\_trigger](https://www.lhc-closer.es/taking_a_closer_look_at_lhc/0.lhc_trigger)  
546

- 547 [87] WLCG Project Office, “Documents & Reference - Tiers - Structure,”  
 548 (2014). <http://wlcg.web.cern.ch/documents-reference> , last accessed on  
 549 30.01.2018.
- 550 [88] CMS Collaboration. “CMSSW Application Framework”, [https:](https://twiki.cern.ch/twiki/bin/view/CMSPublic/WorkBookCMSSWFramework)  
 551 [//twiki.cern.ch/twiki/bin/view/CMSPublic/WorkBookCMSSWFramework](https://twiki.cern.ch/twiki/bin/view/CMSPublic/WorkBookCMSSWFramework),  
 552 last accesses 06.02.2018
- 553 [89] A. Buckleya, J. Butterworthb, S. Giesekec, et. al. “General-purpose event gen-  
 554 erators for LHC physics”. arXiv:1101.2599v1 [hep-ph] 13 Jan 2011
- 555 [90] A. Quadt. “Top Quark Physics at Hadron Colliders”. Advances in the Physics  
 556 of Particles and Nuclei. Springer-Verlag Berlin Heidelberg. DOI: 10.1007/978-  
 557 3-540-71060-8 (2007)
- 558 [91] DurhamHep Data Project, “The Durham HepData Project - PDF Plotter.”  
 559 <http://hepdata.cedar.ac.uk/pdf/pdf3.html> , last accessed on 02.02.2018.
- 560 [92] G. Altarelli and G. Parisi. “ASYMPTOTIC FREEDOM IN PARTON LAN-  
 561 GUAGE”, Nucl.Phys. B126:298 (1977).
- 562 [93] Yu.L. Dokshitzer. Sov.Phys. JETP 46:641 (1977)
- 563 [94] V.N. Gribov, L.N. Lipatov. “Deep inelastic e p scattering in perturbation the-  
 564 ory”, Sov.J.Nucl.Phys. 15:438 (1972)
- 565 [95] F. Maltoni, G. Ridolfi, and M. Ubiali, “b-initiated processes at the LHC: a  
 566 reappraisal,” Journal of High Energy Physics, vol. 07, p. 022, (2012).
- 567 [96] B. Andersson, G. Gustafson, G. Ingelman and T. Sjostrand, “Parton fragmen-  
 568 tation and string dynamics”, Physics Reports, Vol. 97, No. 2-3, pp. 31-145,  
 569 1983.

- [97] CMS Collaboration, “Event generator tunes obtained from underlying event and multiparton scattering measurements;” *European Physical Journal C*, vol. 76, no. 3, p. 155, (2016).
- [98] J. Alwall et. al., “The automated computation of tree-level and next-to-leading order differential cross sections, and their matching to parton shower simulations,” *Journal of High Energy Physics*, vol. 07, p. 079, (2014).
- [99] T. Sjöstrand and P. Z. Skands, “Transverse-momentum-ordered showers and interleaved multiple interactions,” *European Physical Journal C*, vol. 39, pp. 129–154, (2005).
- [100] S. Frixione, P. Nason, and C. Oleari, “Matching NLO QCD computations with Parton Shower simulations: the POWHEG method,” *Journal of High Energy Physics*, vol. 11, p. 070, (2007).
- [101] S. Agostinelli et al., “GEANT4: A Simulation toolkit,” *Nuclear Instruments and Methods in Physics*, vol. A506, pp. 250–303, (2003).
- [102] J. Allison et.al., “Recent developments in Geant4”, *Nuclear Instruments and Methods in Physics Research A* 835 (2016) 186-225.
- [103] CMS Collaboration “Full Simulation Offline Guide”, <https://twiki.cern.ch/twiki/bin/view/CMSPublic/SWGuideSimulation>, last accessed 04.02.2018
- [104] A. Giammanco. “The Fast Simulation of the CMS Experiment” *J. Phys.: Conf. Ser.* 513 022012 (2014)
- [105] A.M. Sirunyan et. al. “Particle-flow reconstruction and global event description with the CMS detector”, *JINST* 12 P10003 (2017) <https://doi.org/10.1088/1748-0221/12/10/P10003>.

- 593 [106] The CMS Collaboration. “ Description and performance of track and pri-  
 594 mary vertex reconstruction with the CMS tracker”. JINST 9 P10009 (2014).  
 595 doi:10.1088/1748-0221/9/10/P10009
- 596 [107] J. Incandela. “Status of the CMS SM Higgs Search” July 4, 2012. Pdf slides.  
 597 Retrieved from [https://indico.cern.ch/event/197461/contributions/](https://indico.cern.ch/event/197461/contributions/1478917/attachments/290954/406673/CMS_4July2012_Final.pdf)  
 598 [1478917/attachments/290954/406673/CMS\\_4July2012\\_Final.pdf](https://indico.cern.ch/event/197461/contributions/1478917/attachments/290954/406673/CMS_4July2012_Final.pdf)
- 599 [108] P. Billoir and S. Qian, “Simultaneous pattern recognition and track fitting by  
 600 the Kalman filtering method”, Nucl. Instrum. Meth. A 294 219. (1990).
- 601 [109] W. Adam, R. Fruhwirth, A. Strandlie and T. Todorov, “Reconstruction of  
 602 electrons with the Gaussian sum filter in the CMS tracker at LHC”, eConf  
 603 C 0303241 (2003) TULT009 [physics/0306087].
- 604 [110] K. Rose, “Deterministic Annealing for Clustering, Compression, Classification,  
 605 Regression and related Optimisation Problems”, Proc. IEEE 86 (1998) 2210.
- 606 [111] R. Fruhwirth, W. Waltenberger and P. Vanlaer, “ Adaptive Vertex Fitting”,  
 607 CMS Note 2007-008 (2007).
- 608 [112] CMS collaboration, “Performance of CMS muon reconstruction in pp collision  
 609 events at  $\sqrt{s} = 7$  TeV ”, JINST 7 P10002 2012, [arXiv:1206.4071].
- 610 [113] Coco, Victor and Delsart, Pierre-Antoine and Rojo-Chacon, Juan and Soyez,  
 611 Gregory and Sander, Christian, “Jets and jet algorithms”, Proceedings,  
 612 HERA and the LHC Workshop Series on the implications of HERA for LHC  
 613 physics: 2006-2008, pag. 182-204. [http://inspirehep.net/record/866539/](http://inspirehep.net/record/866539/files/access.pdf)  
 614 [files/access.pdf](http://inspirehep.net/record/866539/files/access.pdf), (2009), doi:10.3204/DESY-PROC-2009-02/54

- [114] M. Cacciari, G. P. Salam, and G. Soyez, “The anti- $k_t$  jet clustering algorithm,”  
Journal of High Energy Physics, vol. 04, p. 063, (2008).
- [115] S. Catani, Y. L. Dokshitzer, M. H. Seymour, and B. R. Webber, “Longitudi-  
nally invariant  $K_t$  clustering algorithms for hadron hadron collisions”, Nuclear  
Physics B, vol. 406, pp. 187–224, (1993).
- [116] Y.L. Dokshitzer, G.D. Leder, S. Moretti, and B.R. Webber, “Better jet clustering  
algorithms,” Journal of High Energy Physics, vol. 08, p. 001, (1997).
- [117] B. Dorney. “Anatomy of a Jet in CMS”. Quantum Diaries. June  
1st, 2011. Retrieved from [https://www.quantumdiaries.org/2011/06/01/  
anatomy-of-a-jet-in-cms/](https://www.quantumdiaries.org/2011/06/01/anatomy-of-a-jet-in-cms/)
- [118] The CMS Collaboration. “Event Displays from the high-energy collisions at 7  
TeV”, May 2010, CMS-PHO-EVENTS-2010-007, Retrieved from [https://cds.  
cern.ch/record/1429614](https://cds.cern.ch/record/1429614).
- [119] The CMS collaboration. “Determination of jet energy calibration and transverse  
momentum resolution in CMS”. JINST 6 P11002 (2011). [http://dx.doi.org/  
10.1088/1748-0221/6/11/P11002](http://dx.doi.org/10.1088/1748-0221/6/11/P11002)
- [120] The CMS Collaboration, “Introduction to Jet Energy Corrections at  
CMS”. <https://twiki.cern.ch/twiki/bin/view/CMS/IntroToJEC>, last ac-  
cessed 10.02.2018.
- [121] CMS Collaboration Collaboration. “Identification of b quark jets at the CMS  
Experiment in the LHC Run 2”. Tech. rep. CMS-PAS-BTV-15-001. Geneva:  
CERN, (2016). <https://cds.cern.ch/record/2138504>.

- 637 [122] CMS Collaboration Collaboration. “Performance of missing energy reconstruc-  
 638 tion in 13 TeV pp collision data using the CMS detector”. Tech. rep. CMS-PAS-  
 639 JME16-004. Geneva: CERN, 2016. <https://cds.cern.ch/record/2205284>.
- 640 [123] CMS Collaboration, “New CMS results at Moriond (Electroweak) 2013”,  
 641 Retrieved from [http://cms.web.cern.ch/sites/cms.web.cern.ch/files/](http://cms.web.cern.ch/sites/cms.web.cern.ch/files/styles/large/public/field/image/HIG13004_Event01_0.png?itok=LAWZzPHR)  
 642 [styles/large/public/field/image/HIG13004\\_Event01\\_0.png?itok=](http://cms.web.cern.ch/sites/cms.web.cern.ch/files/styles/large/public/field/image/HIG13004_Event01_0.png?itok=LAWZzPHR)  
 643 [LAWZzPHR](http://cms.web.cern.ch/sites/cms.web.cern.ch/files/styles/large/public/field/image/HIG13004_Event01_0.png?itok=LAWZzPHR)
- 644 [124] CMS Collaboration, “New CMS results at Moriond (Electroweak) 2013”,  
 645 Retrieved from [http://cms.web.cern.ch/sites/cms.web.cern.ch/](http://cms.web.cern.ch/sites/cms.web.cern.ch/files/styles/large/public/field/image/TOP12035_Event01.png?itok=uMdnSqzC)  
 646 [files/styles/large/public/field/image/TOP12035\\_Event01.png?itok=](http://cms.web.cern.ch/sites/cms.web.cern.ch/files/styles/large/public/field/image/TOP12035_Event01.png?itok=uMdnSqzC)  
 647 [uMdnSqzC](http://cms.web.cern.ch/sites/cms.web.cern.ch/files/styles/large/public/field/image/TOP12035_Event01.png?itok=uMdnSqzC)
- 648 [125] K. Skovpen. “Event displays highlighting the main properties of heavy flavour  
 649 jets in the CMS Experiment”, Aug 2017, CMS-PHO-EVENTS-2017-006. Re-  
 650 trieved from <https://cds.cern.ch/record/2280025>.
- 651 [126] G. Cowan. “Topics in statistical data analysis for high-energy physics”.  
 652 arXiv:1012.3589v1
- 653 [127] A. Hoecker et al., “TMVA-Toolkit for multivariate data analysis”  
 654 arXiv:physics/0703039v5 (2009)
- 655 [128] L. Lista. “Statistical Methods for Data Analysis in Particle Physics”, 2nd  
 656 ed. Springer International Publishing. (2017) [https://dx.doi.org/10.1007/](https://dx.doi.org/10.1007/978-3-319-62840-0)  
 657 [978-3-319-62840-0](https://dx.doi.org/10.1007/978-3-319-62840-0)

- 658 [129] I. Antcheva et al., “ROOT-A C++ framework for petabyte data storage, sta-  
 659 tistical analysis and visualization ,” Computer Physics Communications, vol.  
 660 182, no. 6, pp. 1384–1385, (2011).
- 661 [130] Y. Coadou. “Boosted decision trees”, ESIPAP, Archamps, 9 Febru-  
 662 ary 2016. Lecture. Retrieved from [https://indico.cern.ch/event/](https://indico.cern.ch/event/472305/contributions/1982360/attachments/1224979/1792797/ESIPAP_MVA160208-BDT.pdf)  
 663 [472305/contributions/1982360/attachments/1224979/1792797/ESIPAP\\_](https://indico.cern.ch/event/472305/contributions/1982360/attachments/1224979/1792797/ESIPAP_MVA160208-BDT.pdf)  
 664 [MVA160208-BDT.pdf](https://indico.cern.ch/event/472305/contributions/1982360/attachments/1224979/1792797/ESIPAP_MVA160208-BDT.pdf)
- 665 [131] J.H. Friedman. “Greedy function approximation: A gradient boosting ma-  
 666 chine”. Ann. Statist. Volume 29, Number 5 (2001), 1189-1232. [https://](https://projecteuclid.org/download/pdf_1/euclid.aos/1013203451)  
 667 [projecteuclid.org/download/pdf\\_1/euclid.aos/1013203451](https://projecteuclid.org/download/pdf_1/euclid.aos/1013203451).
- 668 [132] F. James, M. Roos, “MINUIT: Function minimization and error analysis”. Cern  
 669 Computer Centre Program Library, Geneve Long Write-up No. D506, 1989
- 670 [133] J. Neyman and E. S. Pearson, “On the problem of the most efficient tests of  
 671 statistical hypotheses”. Springer-Verlag, (1992).
- 672 [134] S. S. Wilks, “The Large-Sample Distribution of the Likelihood Ratio for Test-  
 673 ing Composite Hypotheses”, Annals of Mathematical Statistics, vol. 9, pp.  
 674 60–62, (03, 1938).
- 675 [135] A.L. Read. “Modified frequentist analysis of search results (the  $CL_s$  method),”  
 676 (2000). CERN-OPEN-2000-205.
- 677 [136] C. Palmer. “Searches for a Light Higgs with CMS”, CMS-CR-2012-215. [https:](https://cds.cern.ch/record/1560435)  
 678 [//cds.cern.ch/record/1560435](https://cds.cern.ch/record/1560435).



- [137] B. Hespel, F. Maltoni, and E. Vryonidou, “Higgs and Z boson associated production via gluon fusion in the SM and the 2HDM”, JHEP 06 (2015) 065, [https://dx.doi.org/10.1007/JHEP06\(2015\)065](https://dx.doi.org/10.1007/JHEP06(2015)065), arXiv:1503.01656.
- [138] ATLAS Collaboration, “Measurements of Higgs boson production and couplings in diboson final states with the ATLAS detector at the LHC”, Phys. Lett. B726 (2013) 88–119, doi:10.1016/j.physletb.2014.05.011,10.1016/j.physletb.2013.08.010, arXiv:1307.1427. [Erratum: Phys. Lett.B734,406(2014)].
- [139] CMS Collaboration, “Search for the associated production of a Higgs boson with a single top quark in proton-proton collisions at  $\sqrt{s} = 8$  TeV”, JHEP 06 (2016) 177, doi:10.1007/JHEP06(2016)177, arXiv:1509.08159.
- [140] B. Stieger, C. Jorda Lope et al., “Search for Associated Production of a Single Top Quark and a Higgs Boson in Leptonic Channels”, CMS Analysis Note CMS AN-14-140, 2014.
- [141] M. Peruzzi, C. Mueller, B. Stieger et al., “Search for ttH in multilepton final states at  $\sqrt{s} = 13$  TeV”, CMS Analysis Note CMS AN-16-211, 2016.
- [142] CMS Collaboration, “Search for H to bbar in association with a single top quark as a test of Higgs boson couplings at  $\sqrt{s} = 13$  TeV”, CMS Physics Analysis Summary CMS-PAS-HIG-16-019, 2016.
- [143] CMS Collaboration, “Search for production of a Higgs boson and a single top quark in multilepton final states in proton collisions at  $\sqrt{s} = 13$  TeV”, CMS Physics Analysis Summary CMS-PAS-HIG-17-005, 2016.

- 701 [144] B. WG, “BtagRecommendation80XReReco”, February, 2017. <https://twiki.cern.ch/twiki/bin/view/CMS/BtagRecommendation80XReReco>.
- 702
- 703 [145] CMS Collaboration, “Identification of b quark jets at the CMS Experiment  
704 in the LHC Run 2”, CMS Physics Analysis Summary CMS-PAS-BTV-15-001,  
705 2016.
- 706 [146] M. Peruzzi, F. Romeo, B. Stieger et al., “Search for ttH in multilepton final  
707 states at  $\sqrt{s} = 13$  TeV”, CMS Analysis Note CMS AN-17-029, 2017.
- 708 [147] CMS Collaboration, “Baseline muon selections for Run-II.” <https://twiki.cern.ch/twiki/bin/view/CMSPublic/SWGuideMuonIdRun2>, last accessed on  
709  
710 24.02.2018.
- 711 [148] G. Petrucciani and C. Botta, “Two step prompt muon identification”, January,  
712 2015. <https://indico.cern.ch/event/368007/contribution/2/material/slides/0.pdf>.
- 713
- 714 [149] H. Brun and C. Ochando, “Updated Results on MVA eID with 13 TeV samples”,  
715 October, 2014. <https://indico.cern.ch/event/298249/contribution/3/material/slides/0.pdf>.
- 716
- 717 [150] K. Rehermann and B. Tweedie, “Efficient Identification of Boosted Semileptonic  
718 Top Quarks at the LHC”, JHEP 03 (2011) 059, [https://dx.doi.org/10.1007/JHEP03\(2011\)059](https://dx.doi.org/10.1007/JHEP03(2011)059), arXiv:1007.2221.
- 719
- 720 [151] CMS Collaboration. “Tag and Probe”, <https://twiki.cern.ch/twiki/bin/view/CMSPublic/TagAndProbe>, last accessed on 02.03.2018.
- 721
- 722 [152] B. Maier, “SingleTopHiggProduction13TeV”, February, 2016. <https://twiki.cern.ch/twiki/bin/viewauth/CMS/SingleTopHiggsGeneration13TeV>.
- 723